

# Temperature dependence of the fluctuation of the switching field in small magnetic structures

Han-Ting Wang,<sup>1,2</sup> S. T. Chui,<sup>1</sup> A. Oriade,<sup>1</sup> and J. Shi<sup>3</sup>

<sup>1</sup>*Bartol Research Institute, University of Delaware, Newark, Delaware 19716, USA*

<sup>2</sup>*Institute of Physics & Center for Condensed Matter Physics, Chinese Academy of Sciences, Beijing 100080, People's Republic of China*

<sup>3</sup>*Department of Physics, University of Utah, Salt Lake City, Utah, 84112 USA*

(Received 24 October 2003; published 19 February 2004)

We study the temperature dependence of the fluctuation of the switching field of small magnetic structures. For samples of different thicknesses, the fluctuations exhibit *opposite* temperature dependences. At the same time the switching field *decreases* linearly with temperature for both samples. Simulation shows that the mechanism of switching is different between the samples. We perform analytic calculations based on models suggested by the simulation and found temperature dependences in agreement with the experimental results.

DOI: 10.1103/PhysRevB.69.064417

PACS number(s): 75.60.Ej, 75.60.Nt, 75.70.-i

## I. INTRODUCTION

Nanomagnetic structures are currently being developed for magnetic sensors (for example, exploiting the giant magnetoresistance effect, or tunneling magnetoresistance) for nonvolatile magnetic random access memories (MRAM) exploiting either the Hall effect or magnetotransport effects and for storage on a nanoscale. They present challenges in design for controlling the value and reproducibility of the switching field. Both individual and small arrays of MRAM devices have been demonstrated to have a fast access speed ( $\approx 2$  ns), low power consumption, density scalability, and compatibility with semiconductor processing. Since MRAM is inherently nonvolatile, it can potentially enhance or replace existing semiconductor memory devices such as FLASH, SRAM, and DRAM.

In comparison with the mature hard disk or semiconductor memory technology, however, MRAM is still in its infancy. The industrial research laboratories are confronted with many technical challenges ranging from circuit design, processing, testing, packaging, and so on. But nothing is more pressing than solving the magnetic switching problems. These practical problems are intertwined with fundamental micromagnetics. For example, in a functional high-density MRAM chip, 100% bit selectivity is required. Less than 100% selectivity means a poor yield and therefore a high production cost. High bit selectivity means a high degree of control of magnetic switching in millions of MRAM devices. While the industrial research laboratories are gaining success in many technical areas, however, full selectivity in a large array (megabyte array) has not been achieved. On the other hand, the poor selectivity is not a simple process control issue as it is in semiconductor memory technology. It is related with magnetic switching anomalies, which in turn is due to the presence of microscopic magnetization configurations. The solution to this problem requires an in-depth understanding of the micromagnetics. In this paper, we study the fluctuation of the switching field as a function of temperature in nanostructures.

We found that for samples with thicknesses of 200 Å, the switching field fluctuation  $\sigma$  increases with temperature. This is illustrated in Fig. 1 where we show the fluctuation of the switching field  $\sigma$  normalized by the switching field  $H_c$  as

a function of temperature. On the other hand for samples of thicknesses of 100 Å,  $\sigma$  *decreases* with temperature. This is illustrated in Fig. 2 where we show the fluctuation of the switching field  $\sigma$  (+) and the switching field  $H_c/3$  ( $\star$ ) as a function of temperature. (Because the behavior of  $\sigma$  and  $H_c$  is similar, their ratio would not show much temperature dependence. Thus we have not plotted this ratio in this graph.)  $\sigma$  exhibits *opposite* temperature dependences for these two samples. In contrast, the switching field for these samples *always decreases* approximately linearly with temperature.<sup>1,2</sup> Simulation of the micromagnetics provides for snapshots of the magnetization configurations during the switching process in addition to the finite field magnetization configuration before the onset of switching. The simulation suggests that the finite field steady-state configurations before the onset of switching to be similar for these high aspect ratio (5) samples and consists of edge domains. An example of this is shown in Fig. 3. A snapshot of the configurations *during* the switching suggests the mechanism of switching to be different for these two samples, even though the configuration before the onset of switching looks the same for both samples. For the first case, the switching is initiated through the nucleation of a vortexlike nucleus, as is shown in Fig. 4.

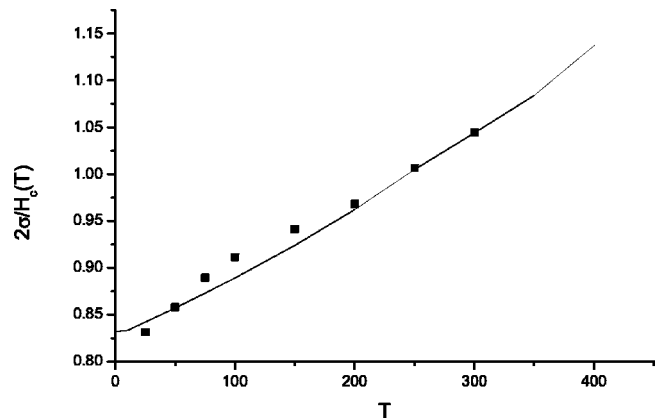


FIG. 1. The fluctuation of the switching field normalized by the switching field of small magnetic structures as a function of temperature. The structure consists of arrays of permalloys of dimension  $0.2 \mu\text{m} \times 1 \mu\text{m} \times 200 \text{Å}$ . The symbols are the experimental results. The line is the theoretical prediction.

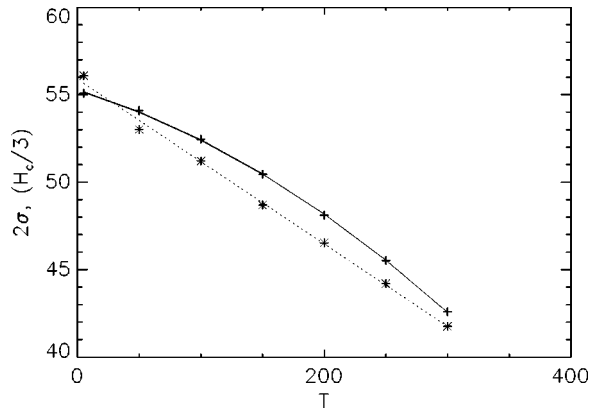


FIG. 2. The switching field  $H_c$  and the fluctuation of the switching field,  $2\sigma$ , of small magnetic structures as a function of temperature. The structure consists of arrays of permalloys of dimension  $0.2 \mu\text{m} \times 1 \mu\text{m} \times 100 \text{ \AA}$ . The symbols are the experimental results. The lines are the theoretical predictions.

For the second case, the edge domain wall is depinned from the sides of the sample, as is shown in Fig. 5. Simulations for different field strengths suggest that the transition between the two mechanisms occurs for a thickness between 200 and 225  $\text{\AA}$ . Garcia and co-workers<sup>3</sup> have performed MFM imaging on permalloy elements of lower aspect ratio (less than or equal to 3) at different field strengths. They found that the domain pattern is affected by the magnetic tip of the MFM. Two different kinds of patterns were observed for samples of the same dimension. Our result differs from theirs in several aspects. First of all, our aspect ratio is larger. Second, the differences we observe occur only during the onset of switching. Because the switching usually takes a nanosecond, it is not possible to observe experimentally the magnetic configurations during the switching process. Finally, the differences observed by Garcia is for the same type of sample whereas the differences reported here are for samples of different thicknesses. We performed analytic calculations for fluctuation for the two different switching mechanisms and

were able to obtain the opposite temperature dependences. The fits to the experimental results are shown by the lines in Figs. 1 and 2. We now describe our results in detail.

## II. 200 $\text{\AA}$ THICK FILMS

The experiments are carried out on NiFe films patterned to arrays consisting of  $200 \text{ nm} \times 1000 \text{ nm}$  identical elements using electron-beam lithography and ion milling. The magnetization measurements were performed using a superconducting quantum interference device magnetometer. In regular magnetic hysteresis the reversible magnetization due to the magnetization rotation would make the apparent switching field distribution broader. In order to eliminate the reversible magnetization contribution, magnetization remanence  $M$  was measured.<sup>8</sup> The  $dM/dH$  curve was then fitted to a Gaussian. Both the mean field and the standard deviation,  $\sigma$ , were obtained for different temperatures. We next turn our attention to our explanation of these phenomena.

First we discuss the case of the thicker samples, where the effect of nucleation is important. The thicknesses of our samples are much smaller than the magnetic length of permalloy (of the order of a micrometer). The spins perpendicular to the sample plane are parallel to each other and are treated as belonging to a single block spin. Thus we can consider the sample as two dimensional. We first explain why vortex formation is more important in thicker films. For thin films, the spins perpendicular to the film plane line up and form a block spin. The magnetization  $M$  per block spin is thus proportional to the thickness  $t$  of the sample; the dipolar interaction between the block spins is proportional to  $M^2$  and hence to  $t^2$ . In contrast the other interaction energy of a block spin such as the exchange, the anisotropy, and the interaction energy with an external magnetic field  $H$  is proportional to  $t$ . The dipolar energy favors the formation of structures with a minimum amount of free magnetic charges such as vortices. It is this increasing importance of the dipolar interaction that leads to the nucleation of a vortexlike

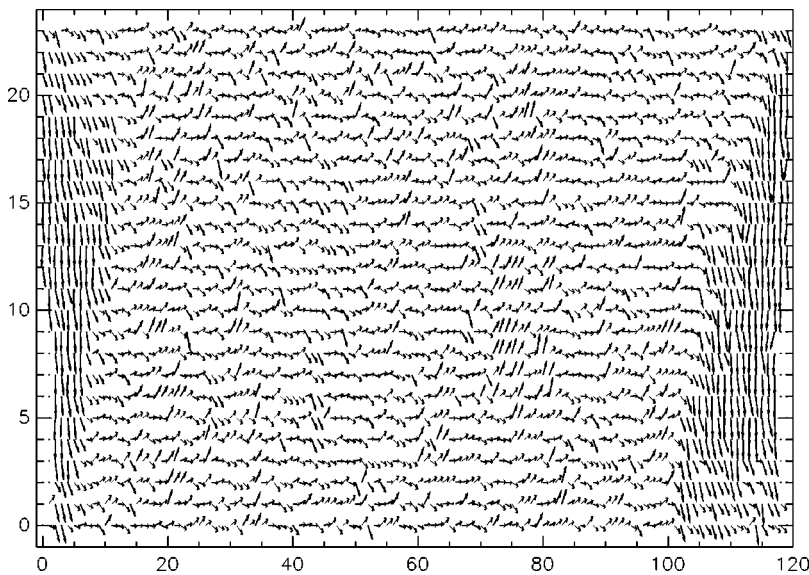


FIG. 3. A snapshot of the steady-state spin configuration at a field ( $H/H_c = 0.925$ ) near the onset of switching for parameters corresponding to that of Fig. 1. The results are obtained from Monte Carlo simulations.

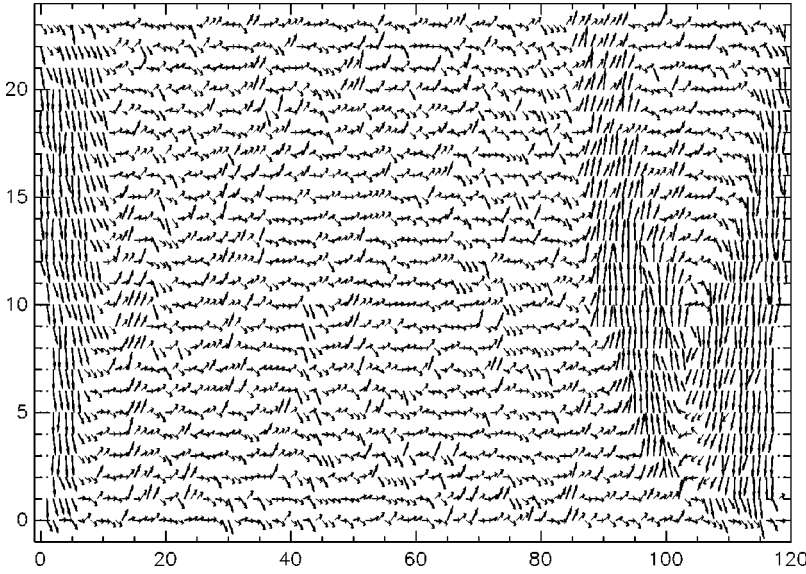


FIG. 4. A spin configuration during the switching for parameters corresponding to that of Fig. 1. The results are obtained from Monte Carlo simulations.

nucleus in thicker films. We next discuss the physics of the nucleation process.

At finite temperatures, the switching usually occurs through thermal activation over a barrier such as nucleation. For materials with macroscopic dimensions, many nucleation centers occur and the average over these centers determines the switching field. When the sample size becomes small enough, only one nucleus occurs within the sample. The occurrence of this nucleus is a random process with a probability determined by the laws of statistical mechanics. Thus there is an intrinsic fluctuation of the switching field. This fluctuation can be called mesoscopic because there usually is only one nucleus and it is not possible to average over many nuclei.

Let  $w(H_c^0, H, T)$  denote the probability of forming a nucleus at magnetic field  $H$  and temperature  $T$ . The probability that the switching field occurs between  $H$  and  $H + dH$  is given by the product of the probability that the switching has not yet occurred times the probability that it will occur in this field range, i.e.,<sup>4</sup>

$$p(H_c^0, H, T) = \left[ 1 - \int_0^H p(H_c^0, H', T) dH' \right] w(H_c^0, H, T). \quad (1)$$

The solution of this equation is

$$p(H_c^0, H, T) = w(H_c^0, H, T) \exp\left(-\int_0^H w(H_c^0, H', T) dH'\right). \quad (2)$$

For a thin magnetic film, the nucleation barrier is generally of the functional form  $E_b = C(H_c^0 - H)^\alpha$ , where  $H_c^0$  is the zero-temperature switching field and  $C$  a constant scaling with the thickness of the film. When the external field is along the easy axis of the sample,  $\alpha = 1$ .<sup>1</sup> The switching probability is thus given by a Boltzmann distribution  $w(H_c^0, H, T) = a \exp(-E_b/k_B T)$ . Carrying out the integral in Eq. (2), the distribution function of the switching field is then

$$p_1(H_c^0, H, T) = a_1 e^{f_1(H)}, \quad (3)$$

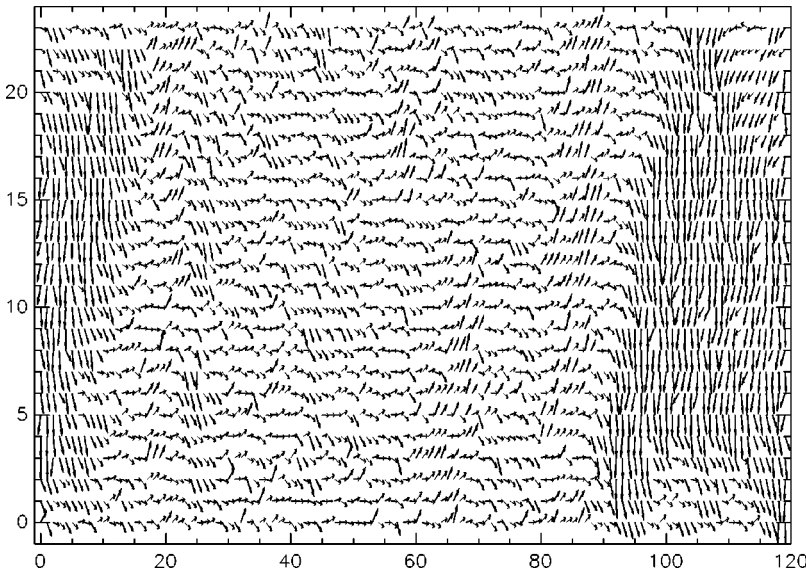


FIG. 5. A snapshot of the spin configuration during the switching for parameters corresponding to that of Fig. 2. The results are obtained from Monte Carlo simulations.

with  $f_1(H) = -\beta C_1(H_c^0 - H) + (a_1/\beta C_1)e^{-\beta C_1 H_c^0} - (a_1/\beta C_1)e^{-\beta C_1(H_c^0 - H)}$ . The integrals for the average  $\langle H^n \rangle = \int p H^n$  can be obtained via the saddle-point method. From  $[\partial f_1(H)]/\partial H = 0$ , we get the point  $H_{c1}(T)$  with the maximum probability:  $H_{c1}(T) = H_c^0 - (1/\beta C_1) \ln a_1/\beta C_1$ . Expanding  $f_1(H)$  around  $H_{c1}(T)$ , we have  $f_1(H) = f_1(H_{c1}) - \frac{1}{2} \beta^2 C_1^2 (H - H_{c1})^2$ . Thus the switching field distribution function is Gaussian and the Gaussian width is  $\sigma_1 = (k_B/C_1)T$ .  $H_{c1}(T)$  is approximately equal to the average switching field  $\langle H \rangle$ . From this, the mean switching field and its *intrinsic* fluctuation shown is obtained.

In real materials, *extrinsic* effects such as impurity effects, edge effects will also affect the switching transition. We incorporate these effects phenomenologically by assuming a Gaussian distribution  $g$  for the zero-temperature switching field  $H_c^0$  with a width  $b$  that can be adjusted,  $g(H_c^0) \propto e^{-(H_c^0 - H_a)/2b^2}$ . The averaged distribution function of the switching field are then

$$q_1(H, T) = \int_0^\infty g(H_c^0) p_1(H_c^0, H, T) dH_c^0. \quad (4)$$

The averaged switching field and the Gaussian width can be calculated numerically,

$$H_c(T) = \int_0^\infty H q_1(H, T) dH, \quad (5)$$

$$(\delta H_c)^2 = \int_0^\infty H^2 q_1(H, T) dH - H_c(T)^2.$$

From these, the solid line in Fig. 1 is obtained. ( $H_a = 300$  Oe,  $b = 130$  Oe,  $a = 10^{14}$ , and  $C = 2 \times 10^{-14}$ .)

When the external field is oriented at a finite angle with respect to the easy axis, in the expression for the nucleation barrier  $E_b$ , the exponent  $\alpha = 1/2$ .<sup>5</sup> In this case,  $w_2(H_c^0, H, T) = a_2 e^{-\beta C_2 (H_c^0 - H)^{1/2}}$ . Substituting this into Eq. (2), we obtain

$$p_2(H_c^0, H, T) = a_2 e^{f_2(H)}, \quad (6)$$

with

$$f_2(H) = -\beta C_2 (H_c^0 - H)^{1/2} + (2a_2/\beta^2 C_2^2) \times e^{\beta C_2 \sqrt{H_c^0}} (\beta C_2 \sqrt{H_c^0} + 1) - (2a_2/\beta^2 C_2^2) \times e^{-\beta C_2 (H_c^0 - H)^{1/2}} [\beta C_2 (H_c^0 - H)^{1/2} + 1].$$

We find that the average switching field decreases with a  $T^2$  proportionality and the Gaussian width  $\sigma_2(T) \propto T^2$ . We next turn our attention to the thinner film case.

### III. THINNER FILMS

The physics of interfaces have witnessed tremendous activity over the last twenty years. The pinning of domain walls in two dimensions has been discussed in the context of the roughening transition previously.<sup>6</sup> We shall study the de-

pinning of the edge domain wall following the formalism developed in this work. We discretize the  $y$  dimension into  $N$  sites separated by a distance  $a$  and approximate the configuration of the domain wall by specifying the height  $\{h_i\}$  at distance  $ia$  from the  $y$  edge of the sample. The energy of the domain wall is described by

$$E(\{h_i\}) = \sum_i^N [f(|h_i - h_{i+1}|) + V(h_i - \delta x_i)], \quad (7)$$

where  $f = \kappa(h_i - h_{i+1})^2/2$  comes from the surface tension of the domain wall;  $V = V_0 - hH$  where  $V_0$  is the pinning potential of the wall and  $H$  is the external magnetic field; and  $\delta x_i$  denotes the roughness of the edge. Numerical estimates<sup>7</sup> suggests that  $V_0$  comes from a domain-wall energy and a dipolar contribution which is of much shorter range.

First we study the straight edge case with the fluctuation  $\delta x_i = 0$ . At zero temperature the equilibrium position  $h_0$  of the domain wall is determined by the equation  $V'(h^0) = H$ . We expand the energy to second order in the change of the wall position  $\delta h$  from this equilibrium position. We obtain  $E = \sum_q |\delta h_q|^2 \omega_q^2$  where  $h_q = \sum_j \exp(iqj) h_j$  and  $\omega_q^2 = \kappa q^2 + V''(h_i^0)/2$ . The depinning instability occurs when  $\omega_q = 0$ . This implies

$$V''(h_c^0) = 0. \quad (8)$$

From this the critical field can be obtained.

We next look at the temperature dependence. The new equilibrium position  $h_i^0(T)$  is now determined by  $\langle V'(h_i^0(T)) \rangle_T = H$  where the angular brackets with a subscript  $T$  indicate thermal averages. Similarly, the critical field is determined from the equation

$$\langle V''(h_i^0(T)) \rangle_T = 0. \quad (9)$$

At low temperatures the thermal averages can be obtained as follows. We write  $h = h^0 + \delta h$ , where  $\delta h$  is from the thermal fluctuation. The thermal averages are then taken with respect to  $\delta h$ . For example,  $\langle V''(h^0) \rangle_T = V''(h^0) + V'''(h^0) \langle \delta h \rangle_T + 0.5 V''''(h^0) \langle (\delta h)^2 \rangle_T$ . In general  $\langle \delta h \rangle_T = 0$  and  $\langle \delta h^2 \rangle_T \propto T$ . From this we find that the changes of both  $h_0$  and  $H_c$  are linear functions of temperature. Similarly, keeping the next order provides an additional correction proportional to  $T^2$ . This change is a sum of two terms, one from the change of  $h_0$ , the other from the difference between  $V'$  and  $\langle V' \rangle$ .

We next incorporate the effect of rough edges so that  $\delta x_i \neq 0$ . First we discuss the zero-temperature situation. We expand the new equilibrium positions of the domain wall around the zero-temperature value and write it as  $h_c^0 + \delta h_i^0$ . The magnetic field is written as  $H = H_c + \delta H$ . The domain-wall positions are determined by  $V'(h_c^0 + \delta h_i^0 - \delta x_i) - H_c - \delta H + \kappa(2\delta h_i^0 - \delta h_{i+1}^0 - \delta h_{i-1}^0) = 0$ . Expanding  $V$ , we get

$$(\delta h_i^0 - \delta x_i)^2 V'''/2 + \kappa(2\delta h_i^0 - \delta h_{i+1}^0 - \delta h_{i-1}^0) - \delta H = 0. \quad (10)$$

The  $V'(h_0)$  term is canceled by  $H$ ;  $V''(h_0) = 0$ .

We now solve this equation with a mean-field approximation. Let us call the mean value  $\langle \delta h_i^0 \rangle = dh$ . Equation (6)

reduces to the following equation:  $(dh \delta h_i^0 - 2dh \delta x_i + \delta x_i^2) V''' - \delta H + \kappa(2\delta h_i^0 - \delta h_{i+1}^0 - \delta h_{i-1}^0) = 0$ . The solution of this can be carried out in Fourier space and is given by  $\delta h_q^0 = [-2dh(\delta x)_q + (\delta x^2)_q - \delta H'] / (\kappa' q^2 + dh)$ , where  $\kappa' = \kappa / V'''$  and  $\delta H' = \delta H / V'''$ . From this we obtain the self-consistent equation for  $dh$ :  $dh^2 - 2dh \delta \bar{x} + \delta \bar{x}^2 - \delta H / V''' = 0$ . We get

$$\langle \delta h_i^0 \rangle = \delta \bar{x} \pm [(\delta \bar{x})^2 - \delta \bar{x}^2 + \delta H / V''']^{0.5}, \quad (11)$$

where  $\delta \bar{x} = (\sum_i \delta x_i / N)$  and  $\delta \bar{x}^2 = (\sum_i \delta x_i^2 / N)$ . The angular brackets indicate impurity averages.

Again the switching field is determined from the condition that the lowest normal-mode frequency is equal to zero. The normal-mode frequency is determined from the energy change  $\delta E$  of the system when the domain-wall positions are changed by  $\delta h_i$ . They are determined by the energy change  $V''(h_0 + \delta h_i^0 - \delta x_i) \delta h_i^2 / 2 + \kappa(\delta h_i - \delta h_{i+1})^2$ . We get  $E = E_0 + \delta E$ , where  $H_0 = \sum_i V''(h_i^0) \delta h_i^2 + \kappa(\delta h_i - \delta h_{i+1})^2$  and  $\delta E = \sum_q \kappa q^2 |\delta h_q|^2 \sum_i (\delta h_i^0 - \delta x_i) V'''(h_0) \delta h_i^2$ . The change of the energy can be determined from perturbation theory as  $\Delta E = \langle 0 | \delta E | 0 \rangle$ . From this we obtain the equation  $\langle \delta h \rangle = \delta \bar{x}$ .

The quantity under the square-root sign in Eq. (11) must be zero. Generalizing to finite temperatures we find that the change of the switching field at a finite temperature is given by

$$\langle \delta H_c \rangle_T = \langle V''' \rangle_T [\delta \bar{x}^2 - (\delta \bar{x})^2]. \quad (12)$$

As the temperature is increased, the potential softens. Thus both the switching field and its fluctuation decrease with temperature as sums of terms that are linear and quadratic in  $T$ , as is shown in Fig. 2.

In summary, we show that the fluctuations of the switching field exhibit opposite temperature dependences from permalloy structures of different thicknesses. We propose that this is due to different switching mechanisms for the two cases. Analytic calculations are presented to explain these phenomena.

#### ACKNOWLEDGMENTS

This work was supported in part by the NSF Grant No. ECS-0115164.

<sup>1</sup>S.T. Chui, J. Magn. Magn. Mater. **168**, 9 (1997).

<sup>2</sup>Jian Li, Jing Shi, and Saied Tehrani, Appl. Phys. Lett. **79**, 3821 (2001).

<sup>3</sup>J.M. Garcia, A. Thiaville, J. Miltat, K.J. Kirk, and J.N. Chapman, J. Magn. Magn. Mater. **242-245**, 1267 (2002).

<sup>4</sup>Juhani Kurkijärvi, Phys. Rev. B **6**, 832 (1972); T.A. Fulton and L.N. Dunkleberger, *ibid.* **9**, 4760 (1974); Anupam Garg, Phys.

Rev. B **51**, 15 592 (1995).

<sup>5</sup>H. T. Wang, A. Oriade, S. T. Chui, and J. Shi (unpublished).

<sup>6</sup>S.T. Chui and J.D. Weeks, Phys. Rev. B **23**, 2438 (1981).

<sup>7</sup>S.T. Chui, IEEE Trans. Magn. **34**, 1000 (1998). Figures 6 and 7 of this paper show the change in energy of the system as the edge domain wall is displaced.

<sup>8</sup>Jing Shi and S. Tehrani, Appl. Phys. Lett. **77**, 1692 (2000).